Available online at www.sciencedirect.com

ScienceDirect

Geochimica et Cosmochimica Acta 257 (2019) 68–79

Geochimica et Cosmochimica Acta

www.elsevier.com/locate/gca

Clumped isotopes in land snail shells over China: Towards establishing a biogenic carbonate paleothermometer

Jixuan Zhai [a,b,c,d], Xu Wang [a,b,c,*], Ben Qin [e], Linlin Cui [c,f], Shuhua Zhang [g] Zhongli Ding [a,b,c]

[a] *Key Laboratory of Cenozoic Geology and Environment, Institute of Geology and Geophysics, Chinese Academy of Sciences, P.O. Box 9825, Beijing 100029, China*

[b] *CAS Center for Excellence in Life and Paleoenvironment, Beijing, 100044, China*

[c] *Institutions of Earth Science, Chinese Academy of Sciences, P.O. Box 9825, Beijing 100029, China*

[d] *University of Chinese Academy of Sciences, Beijing 100049, China*

[e] *State Key Laboratory of Geological Processes and Mineral Resources, China University of Geosciences, Beijing 100083, China*

[f] *Institute of Geology and Geophysics, Chinese Academy of Sciences, P.O. Box 9825, Beijing 100029, China*

[g] *Brigade 606 of Sichuan Metallurgical and Geological Exploration Bureau, Chengdu 611730, China*

Received 27 January 2019; accepted in revised form 26 April 2019; Available online 7 May 2019

Abstract

Land snail fossils are abundantly distributed in geological deposits and their isotopic compositions provide a means to determine paleoclimatic changes. With the development of the clumped isotopes (Δ_{47}) geothermometer, many efforts have been made in recent years to study clumped isotopes in land snail shell carbonate. Although there have been several recent attempts, there is, as yet, no empirical calibration function to convert land snail Δ_{47} to environmental temperature. Here, we systematically analyzed clumped isotopes (Δ_{47}) of two common land snail species (*Bradybaena* and *Cathaica*) from China. Results showed that temperatures calculated using the Δ_{47} (T_{47}) of both species did not correlate with the mean annual temperatures (MAT) at the study sites. However, the T_{47}-MAT offset is negatively correlated to MAT, suggesting that land snails tend to add shell during the warmer months at colder sites or modulate their body temperature differently in colder regions. Meanwhile, clumped temperatures of *Cathaica* are 3.4 ± 1.5 °C higher than those of *Bradybaena* at 18 sites, indicating that a species-specific transfer function is needed to reconstruct paleotemperature using land snail clumped isotopes. After determining the proper duration of the growing season for land snails at different locations, we developed a Δ_{47}-growth season temperature (GST) transfer function for the two species. The calibration function for *Bradybaena* land snails is expressed by a linear regression between $1/T^2$ and absolute Δ_{47} ($R^2 = 0.94$): $\Delta_{47} = (0.0513 \pm 0.0036) \times 10^6/T^2 + (0.0930 \pm 0.0413)$, where Δ_{47} is expressed in ‰ and T in K. The calibration function for *Cathaica* is as follows ($R^2 = 0.80$): $\Delta_{47} = (0.055 \pm 0.011) \times 10^6/T^2 + (0.035 \pm 0.129)$. The function for *Cathaica* was successfully applied to reconstruct mean summer (June-July-August) temperatures during the Last Glacial Maximum and modern times on the central Chinese Loess Plateau, based on Δ_{47} data of *Cathaica* sp. provided by Eagle et al (2013a). This testifies to the validity of the aforementioned constructed transfer function. In addition, the calculated $\delta^{18}O$ of body water ($\delta^{18}O_{BW}$) for *Bradybaena* showed a robust correlation with the $\delta^{18}O$ of rainfall ($\delta^{18}O_p$), particularly in northern China, which points to the potential to trace hydrological changes in the region. In contrast, *Cathaica* $\delta^{18}O_{BW}$ did not show a straightforward relation to $\delta^{18}O_p$. This inter-species complexity warrants further study.

Keywords: Clumped isotope; Land snail; *Bradybaena*; *Cathaica*; Δ_{47}-T transfer function; Paleothermometer

* Corresponding author at: Key Laboratory of Cenozoic Geology and Environment, Institute of Geology and Geophysics, Chinese Academy of Sciences, P.O. Box 9825, Beijing 100029, China.

E-mail address: xuking@mail.iggcas.ac.cn (X. Wang).

https://doi.org/10.1016/j.gca.2019.04.028

0016-7037/

1. INTRODUCTION

There are several advantages to studying land snail shells for paleoclimate reconstruction. First, land snails only migrate a short distance and are thus suitable for determining paleoclimate at the local scale (Liu et al., 1985). Second, changes in land snail faunal assemblages are highly sensitive to climatic variation and are thus ideal for studying seasonal changes (Wu et al., 2018). Third, land snail fossils can be abundant in geological deposits throughout the world, allowing for broad application in different regions.

The use of land snail fossils to infer their living environment began during the 1960s (Sparks, 1961; Lozek, 1965) and there has been nearly continuous effort since then. Land snail faunal assemblages have become a powerful tool for showing past environmental or ecological changes (Wu et al., 2018). Stable isotopic study of land snail shells in particular provide further information on vegetation and environmental changes. For example, the carbon isotopic composition of land snail shells is closely related to the proportion of C_3/C_4 plants in their diet (DeNiro and Epstein, 1978; Francey, 1983; Stott, 2002; Metref et al., 2003; Liu et al., 2007). And the oxygen isotope in shell carbonate ($\delta^{18}O_{shell}$) is theoretically governed by $\delta^{18}O$ of snail body water and the temperature at which shell carbonate precipitates, and reflects the influence of environmental variables. For example, $\delta^{18}O_{shell}$ was found to be linked to precipitation in France, Italy, Libya and great plains of USA (Lécolle, 1985; Goodfriend and Ellis, 2002; Prendergast et al., 2015; Zanchetta et al., 2005), to relative humidity in North America (Yapp, 1979; Zaarur et al., 2011), to precipitation in China (Liu et al., 2006), and to temperature in Israel, Spain and North America (Magaritz et al., 1981; Grossman and Ku, 1986; Yanes et al., 2009). The complexity of this relationship may be attributed to variations in regional climatic seasonality and the ecophysiological traits of land snails. Despite the growing use of shell stable isotopes, physical and metabolic processes governing the isotopic composition of land snail shells is complex and remains poorly understood.

Recently, clumped isotopes in carbonate (Δ_{47}) have been developed as a new type of paleothermometer and are defined as the enrichment of $^{13}C^{18}O^{16}O$ in a sample relative to that at an isotopic stochastic distribution (Ghosh et al., 2006). The technique has an advantage over the conventional oxygen isotope geothermometer in that temperature can be directly inferred in the absence of data on $\delta^{18}O$ in the fluid from which the carbonate precipitated. This powerful tool, once applied to land snail shells, has the potential to reconstruct temperature of an environment where snails grew and simplify the complicated interpretation of shell oxygen isotopes through calculating snail body fluid $\delta^{18}O$ based on obtained shell calcification temperature. However, in the first clumped isotope study for land snail shells on a global scale, Zaarur et al. (2011) found no correlation between shell-calcification temperature and environmental temperature. Eagle et al. (2013a) demonstrate the application of land snail shell clumped isotopes to trace ambient temperature in a monsoonal region, and reconstruct temperature and water isotope shifts from the Last Glacial Maximum (LGM) to the present on the Chinese Loess Plateau. Indeed, Wang et al. (2016) show a robust correlation of clumped isotope temperature with environmental temperature for two modern dominant land snail species (*Bradybaena* and *Cathaica*) in North China. More recently, Zhang et al. (2018) strongly suggested that clumped isotopes in land snail shells reach isotopic equilibrium in shell culture studies, in the absence of kinetic or vital effects, which highlights the value of shell clumped isotopes in paleoclimatic studies. Notwithstanding these developments, it remains unclear whether the correlation of land snail clumped isotopes with environmental temperature is applicable over a broad monsoonal region. Moreover, there is still no clumped isotope thermometry for land snails.

In this study, we systematically collected modern land snails (*Bradybaena* and *Cathaica*) over the whole of China over a large gradient of environmental variables (i.e. a mean annual temperature and precipitation change of 20 °C and 2000 mm, respectively) and measured clumped isotopes in these shells. Based on the data, a transfer function of the relationship of land snail shell Δ_{47} to environmental temperature was proposed for the two species. This study provides a foundation to reconstruct paleotemperature and paleohydrology using clumped isotopes of land snail shell carbonate.

2. MATERIALS AND METHODS

2.1. Sample collection

Living land snails were collected during summer and autumn (August–October) of 2016 and 2017, with a small number collected during the period 2013–2015. A total of 64 sites for *Bradybaena* and 24 sites for *Cathaica* were sampled during this period. There were relatively fewer sampling sites for *Cathaica* because they mainly live in northern China given their ecophysiological habits (Fig. 1). The *Bradybaena* land snails include *Bradybaena (Acusta) ravida ravida*, *Bradybaena (B.) similaris similaris*, *Bradybaena (B.) fuchsia* and *Bradybaena (Acusta) ravida sieboldiana*. The *Cathaica* land snails include *Cathaica cunlunensis*, *Cathaica pulveratricula*, *Cathaica (Pliocathaica) pulveratrix*, *Cathaica (Xerocathaica) pekinensis*, *Cathaica (C.) fasiola fasicola*, *Cathaica gansuica*, and *Cathaica sp*. These land snails were collected from greenlands or parks in rural areas or on the outskirts of cities, away from human disturbance. The vegetation at the sampling sites was composed of either trees or shrubs with some understory grasses. The trees are mostly conifers, willows, and poplars whereas the shrubs are typically *Loropetalum chinense var. rubrum*, Symplocaceae, Pittosporum, Nanshan Berberidaceae (bamboo), *Schefflera heptaphylla,* and *Photinia serrulata*. Most are C_3 plants. The sampling sites of *Bradybaena* cover large environmental gradient in China, over a geographical range of 18.3–45.8 °N and 98.3–126.5°E. In contrast, the distribution of *Cathaica* is confined to northern China (i.e. 31.9–41.8°N and 106.8–124.3°E). The mean annual temperature (MAT) for the sampling sites ranges from 5.0-25.2 °C, the mean annual

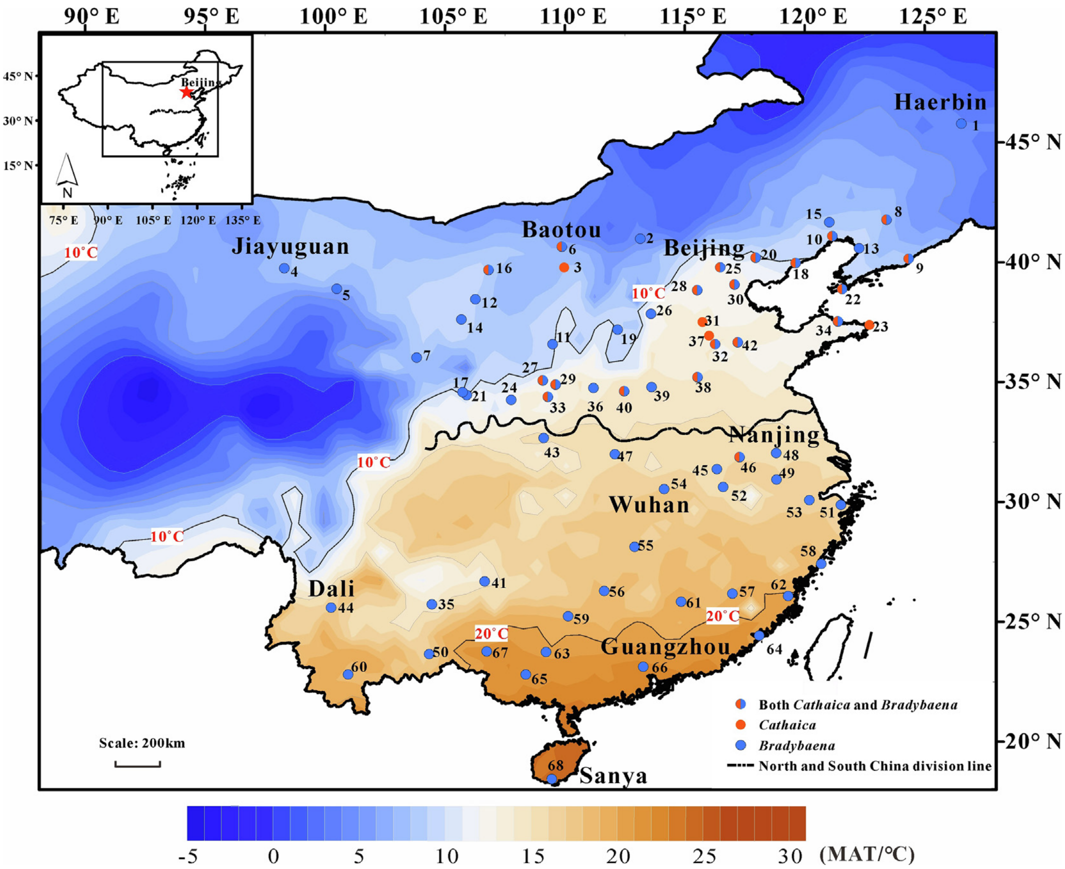

Fig. 1. Location of sampling sites for *Bradybaena* (blue solid circle) and *Cathaica* (red solid circle). (For interpretation of the references to colour in this figure legend, the reader is referred to the web version of this article.)

precipitation (MAP) ranges from 88 to 2129 mm, the mean annual relative humidity (MARH) ranges from 41 to 82%, and the altitude ranges from 3 to 1904 m.

All the meteorological data were provided by the China Meteorological Data Service Center (http://data.cma.cn/en). Dataset of Monthly Surface Observation Values in Individual Years (1981–2010). All MAT and seasonal temperature data were corrected for altitudinal differences between sampling sites and meteorological stations. If there was no meteorological station at a sampling site, data from the nearest meteorological stations were employed.

2.2. Sample pretreatment and clumped isotopic analysis

The organic body parts of living land snails were gently removed in the field in order to keep the shells intact. In the laboratory, all the land snail shells were first cleaned in distilled water using a toothbrush to remove soil particles or organic debris and then cleaned six times using an ultrasonic bath. This procedure produced a clean shell free of any macroscopic contamination. The cleaned shells were then dried at 60 °C overnight. For subsequent clumped isotopic analysis, multiple shells, at least four shells depending on availability (see Table 1), were combined and ground to a fine powder using a pestle and mortar. To ensure the representativeness of each aliquot, the shell powder was homogenized and adequately mixed prior to analysis. The combination of multiple shells at each site ensured that the analyzed sample approximated an average of the existing conditions.

To generate CO_2 for clumped isotopic analysis, an approximately 15 mg aliquot of shell powder was reacted with ~103% phosphoric acid ($\rho = 1.90$ g/cm^3) under a vacuum in a McCrea-type reaction vessel (McCrea, 1950) for approximately 16 h at 25 °C following the method developed by Ghosh et al. (2006). Subsequently, the produced CO_2 was purified by removing trace water and organic and sulfur-bearing contaminants using a prep line following the procedure of Wang et al. (2016). Finally, the purified CO_2 was placed in a MAT 253 (Thermo Scientific) isotope ratio mass spectrometer to measure clumped and stable isotopes by monitoring masses 44–49 (Cui and Wang, 2014). One measurement requires 2.5 h at an analytical precision better than 0.01‰ (SE). For most powdered shell samples, 2–5 replicates were analyzed and a total of 177 Δ_{47} values were obtained (Table EA-3). All the clumped isotope analyses were carried out in the Laboratory for Environmental Isotope Geochemistry, Institute of Geology and Geophysics, Chinese Academy of Sciences.

To determine the growth seasonality of the land snails, we selected a single clean shell from adult land snails from five different sites (Table EA-2) to analyze carbon and oxygen isotopes along the growth band of the shell. A small amount of powder was collected from each shell using a

Table 1
Compiled data of averaged $\delta^{18}O$, Δ_{47} and T_{47} for all samples (data with "underline" were sited from Wang et al. (2016)).

Site no.	Study site	Bradybaena				Cathaica			
		N	$\delta^{18}O_{shell}$(‰) VPDB	Δ_{47} (‰)	T_{47} (°C)	N	$\delta^{18}O_{shell}$(‰) VPDB	Δ_{47} (‰)	T_{47} (°C)
1	Haerbin	4	−5.64	0.675 ± 0.011	33.0 ± 2.4				
2	Wulanchabu	10	−5.51	0.697 ± 0.003	28.1 ± 0.7				
3	Eerduosi					5	−4.16	0.684 ± 0.000	30.9 ± 0.0
4	Jiayuguan	8	0.50	0.687 ± 0.004	30.3 ± 0.9				
5	Zhangye	8	−0.92	0.682 ± 0.003	31.4 ± 0.8				
6	Baotou	8	−3.55	0.688 ± 0.005	30.0 ± 1.1	10	−4.18	0.664 ± 0.011	35.4 ± 2.6
7	Lanzhou	10	0.10	0.696 ± 0.002	28.4 ± 0.3				
8	Shenyang	9	−4.43	0.678 ± 0.006	32.1 ± 1.3	10	−4.40	0.677 ± 0.008	32.5 ± 2.0
9	Dandong	6	−2.89	0.679 ± 0.005	31.9 ± 1.2	10	−5.26	0.675 ± 0.006	32.8 ± 1.4
10	Jinzhou	10	−3.99	0.675 ± 0.001	31.7 ± 2.0	8	−4.02	0.664 ± 0.009	35.4 ± 2.0
11	Yanan	10	−6.64	0.698 ± 0.008	27.8 ± 2.0				
12	Yinchuan	10	−1.95	0.687 ± 0.004	30.3 ± 0.8				
13	Yingkou	10	−3.59	0.678 ± 0.002	32.3 ± 0.4				
14	Zhongning	10	−2.05	0.673 ± 0.014	33.4 ± 3.3				
15	Beipiao	10	−3.20	0.663 ± 0.000	35.7 ± 0.0				
16	Wuhai	10	−2.65			10	−2.29	0.684 ± 0.002	30.9 ± 0.4
17	Ganquan	10	−1.22	0.684 ± 0.008	26.1 ± 2.0				
18	Qinhuangdao	10	−2.87			10	−4.46	0.680 ± 0.007	31.7 ± 1.5
19	Pingyao	8	−3.59	0.695 ± 0.008	28.4 ± 2.0				
20	Jixian	1	−4.21	0.692 ± 0.008	29.0 ± 2.0	2	−5.43	0.670 ± 0.010	34.0 ± 2.8
21	Tianshui	10	−2.09	0.694 ± 0.010	28.722.2				
22	Dalian	10	−1.94	0.692 ± 0.006	29.1 ± 1.3	10	−2.47	0.683 ± 0.010	31.2 ± 2.2
23	Rongcheng					10	−2.75	0.693 ± 0.003	28.8 ± 0.6
24	Meixian	10	−4.86	0.702 ± 0.008	27.1 ± 1.7				
25	Beijing	2	−3.23	0.690 ± 0.009	29.5 ± 2.0	2	−3.51	0.667 ± 0.011	35.0 ± 2.8
26	Yangquan	10	−2.61	0.679 ± 0.000	31.9 ± 0.1				
27	Tongchuan	1	−3.57	0.699 ± 0.009	28.0 ± 2.0	1	−1.71	0.682 ± 0.007	31.0 ± 2.0
28	Dingzhou	1	N.A.	0.686 ± 0.008	30.0 ± 2.0	1	−5.92	0.664 ± 0.008	35.0 ± 2.0
29	Pucheng	3	−5.10	0.694 ± 0.006	28.7 ± 1.2	1	−7.27	0.677 ± 0.007	32.0 ± 2.0
30	Tianjin	2	−4.31	0.687 ± 0.006	30.0 ± 1.1	2	−4.12	0.667 ± 0.004	34.7 ± 1.2
31	Zaoqiang					8	−5.80	0.671 ± 0.008	33.8 ± 2.0
32	Chiping	7	−4.09	0.701 ± 0.017	29.7 ± 1.6	9	−3.84	0.681 ± 0001	31.6 ± 0.2
33	Lintong	1	−1.92	0.681 ± 0.008	32.0 ± 2.0	1	−4.52	0.669 ± 0.007	34.0 ± 2.0
34	Yantai	10	−3.37	0.696 ± 0.014	28.4 ± 2.9	10	−3.83	0.684 ± 0.002	30.9 ± 0.5
35	Panzhou	10	−3.17	0.700 ± 0.007	27.3 ± 1.6				
36	Sanmenxia	10	−1.27	0.695 ± 0.008	28.5 ± 1.8				
37	Xiajin					10	−6.07	0.665 ± 0.005	35.2 ± 1.2
38	Heze	10	−0.95	0.691 ± 0.007	29.3 ± 1.5	10	−5.29	0.675 ± 0.013	32.9 ± 2.8
39	Zhengzhou	10	−2.80	0.678 ± 0.002	32.1 ± 0.5				
40	Luoyang	1	−4.56	0.677 ± 0.008	32.0 ± 2.0	1	−3.00	0.666 ± 0.008	35.0 ± 2.0
41	Guiyang	10	−2.98	0.684 ± 0.026	31.1 ± 5.8				
42	Jinan	9	−2.78	0.684 ± 0.002	30.9 ± 0.5	10	−2.72	0.668 ± 0.009	34.4 ± 2.0
43	Ankang	10	−0.38	0.678 ± 0.002	32.3 ± 0.4				
44	Dali	10	−5.44	0.698 ± 0.008	27.9 ± 2.2				
45	Huoshanxian	10	−3.69	0.683 ± 0.012	31.2 ± 2.6				
46	Hefei	10	−0.93	0.690 ± 0.015	29.5 ± 3.4	10	−3.80	0.674 ± 0.016	34.4 ± 2.3
47	Xiangyang	10	−1.17	0.674 ± 0.001	33.1 ± 0.2				
48	Nanjing	10	0.26	0.677 ± 0.006	32.5 ± 1.4				
49	Xuancheng	10	−1.22	0.673 ± 0.000	33.3 ± 0.0				
50	Wenshan	10	−2.99	0.682 ± 0.008	31.4 ± 2.0				
51	Ningbo	10	−0.47	0.678 ± 0.006	32.3 ± 1.4				
52	Qianshanxian	7	0.66	0.676 ± 0.009	32.8 ± 1.9				
53	Hangzhou	10	−2.64	0.669 ± 0.004	34.3 ± 0.9				
54	Wuhan	10	−1.38	0.671 ± 0.007	33.9 ± 1.6				
55	Changsha	10	−2.30	0.688 ± 0.006	30.0 ± 1.3				
56	Yongzhou	10	−1.62	0.677 ± 0.016	32.5 ± 3.5				
57	Sanming	10	−0.56	0.674 ± 0.005	33.2 ± 1.0				
58	Wenzhou	10	−2.78	0.672 ± 0.001	33.5 ± 0.2				
59	Guilin	10	−4.38	0.674 ± 0.003	33.2 ± 0.7				

Table 1 (*continued*)

Site no.	Study site	N	$\delta^{18}O_{shell}$(‰) VPDB	Δ_{47} (‰)	T_{47} (°C)	N	$\delta^{18}O_{shell}$(‰) VPDB	Δ_{47} (‰)	T_{47} (°C)
60	Puer	10	−3.97	0.671 ± 0.009	33.9 ± 2.1				
61	Ganzhou	10	−3.09	0.670 ± 0.007	34.1 ± 1.7				
62	Fuzhou	10	−1.39	0.693 ± 0.003	28.9 ± 0.6				
63	Laibin	10	−0.81	0.685 ± 0.014	30.6 ± 3.2				
64	Xiamen	10	0.83	0.686 ± 0.008	30.5 ± 1.8				
65	Nanning	10	−5.18	0.670 ± 0.007	34.1 ± 2.0				
66	Guangzhou	10	−2.06	0.673 ± 0.007	33.4 ± 1.4				
67	Baise	10	−6.85	0.678 ± 0.006	32.2 ± 1.2				
68	Sanya	6	−4.23	0.670 ± 0.020	34.3 ± 4.5				

micro-drill along a sampling line perpendicular to the growth direction to represent a short time interval of the snail's life. Sequential sampling was performed along the growth direction from the shell lip to the apex at an interval of less than 2 mm (Fig. 2). At the top of each shell, the size of the growth band was too small to allow collection of sufficient powder for stable isotopic analysis. Stable carbon and oxygen isotopes were measured on each powder sample using a GasBench II linked to a Delta V plus isotope ratio mass spectrometer (Thermo Fisher). Briefly, a powder aliquot of approximately 100 µg was reacted with 100 % H_3PO_4 at 72 °C for 1 h. The resultant CO_2 was purified by passing the sample through two NAFION^{TM} water traps and a PoraPlot Q chromatograph column (maintained at 45 °C) and then placed in the mass spectrometer for isotopic measurement. Carbon and oxygen isotopes were expressed using conventional δ notation and reported relative to the Vienna Pee Dee Belemnite (VPDB) scale. Analytical precisions for $\delta^{13}C$ and $\delta^{18}O$ were 0.15‰ and 0.2‰, respectively.

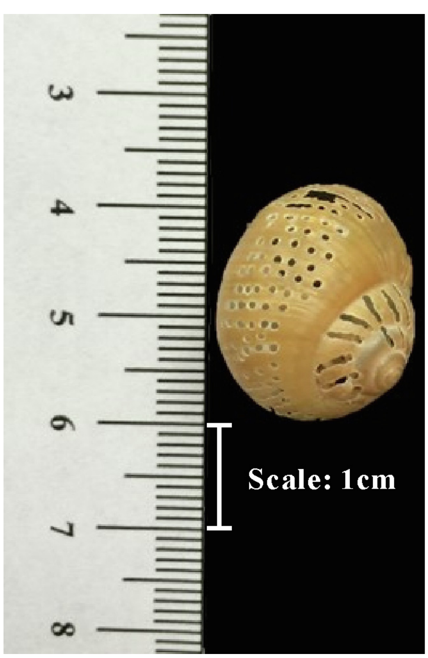

Fig. 2. Photograph showing the sampling scenario along the growth band of a *Bradybaena* shell from Jinan. The minimum scale is 1 mm.

2.3. Data calibration and calculation

All the clumped isotopic data were calibrated using an absolute reference frame following the procedure presented by Dennis et al. (2011). The absolute reference frame was composed of a heated gas line (at 1000 °C) and water equilibrated gas lines at various temperatures (25 °C is usually adopted). To construct a heated gas line, a set of purified CO_2 gases in sealed quartz tubes were heated at 1060 °C in a muffle furnace for 3 h to reach an isotopically random distribution and then quickly cooled to room temperature. To obtain an equilibrated gas line, numerous purified CO_2 gases were sealed together using a small amount of water in glass tubes and then were placed in a water bath at 25 °C to isotopically equilibrate for more than 72 h (Wang et al., 2016). All the heated/equilibrated gases or standard gases were purified using a prep line in the same manner as the sample gases being completed. After calibration using the absolute reference frame in our laboratory, the mean Δ_{47} value of the NBS-19 carbonate standards was 0.383‰, which is comparable to the accepted value of 0.392‰ (Dennis et al., 2011). All the clumped isotopic data were converted to calcification temperatures using the following equation (Dennis et al., 2011):

$$\Delta_{47} = (0.0636 \pm 0.0049 \times 10^6)/T^2 - (0.0047 \pm 0.0520)(1 - 50\,^{\circ}C) \quad (1)$$

This equation was converted from the previous transfer function developed by Ghosh et al. (2006) after presenting the Ghosh Δ_{47} data in the absolute reference frame. The equation defined by Ghosh et al. (2006) is commonly used for clumped isotope temperature calibration particularly in land snail studies (Eagle et al., 2013a; Zaarur et al., 2011). Moreover, Wang et al. (2016) also chose the Eq. (1) to calibrate the clumped isotopes. The choice of this method allows for a direct comparison of our current study to previous studies.

3. RESULTS

All the measured data are shown in Tables 1 and EA-1. Δ_{47} values of the *Bradybaena* shells ranged from 0.663‰ to 0.702‰ (mean: 0.683 ± 0.010‰), corresponding to a temperature (T_{47}) range of 26.1 °C to 35.7 °C (mean: 31.0 ± 2.2 °C). The $\delta^{18}O_{shell}$ (VPDB) was −6.85‰ to + 0.83‰ (mean: −2.73 ± 1.78‰). Based on T_{47} and $\delta^{18}O_{shell}$, we calculated $\delta^{18}O$ in the snail body water ($\delta^{18}O_{BW,}$ Vienna Stan-

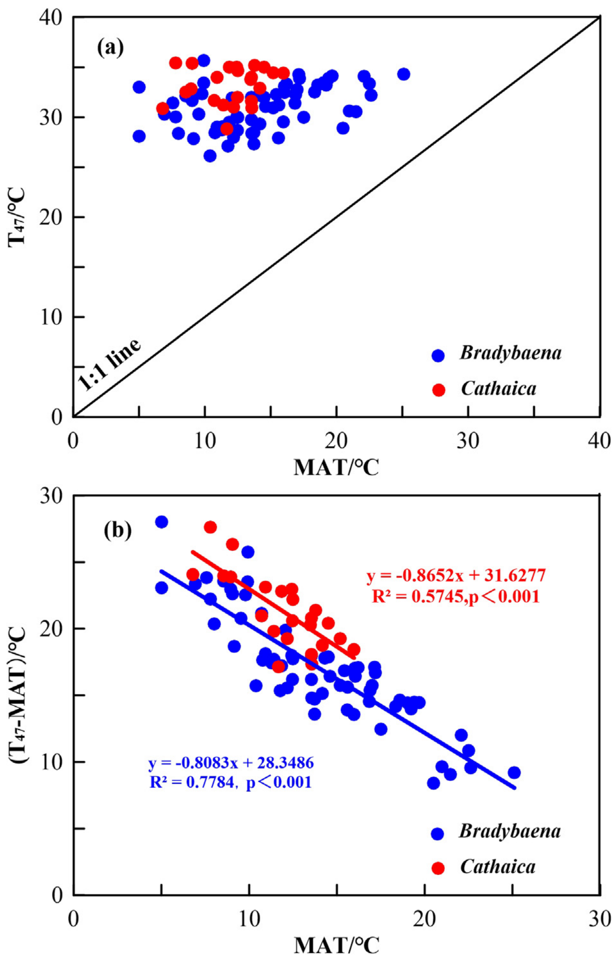

Fig. 3. (a) Crossplot of T_{47} and MAT for *Bradybaena* and *Cathaica* and (b) plot showing a negative correlation between the T_{47}-MAT offset and MAT.

dard Mean Ocean Water [VSMOW]), which ranged from −4.47‰ to + 3.80‰ (mean: 0.07 ± 1.90‰). In contrast, the *Cathaica* land snails have Δ_{47} values between 0.664‰ and 0.693‰ (mean: 0.674 ± 0.008‰) with the corresponding T_{47} value varying from 28.8 °C to 35.4 °C (mean: 32.9 ± 2.0 °C). The $\delta^{18}O_{shell}$ (VPDB) and $\delta^{18}O_{BW}$ (VSMOW) varied from −7.27‰ to −1.71‰ (mean: −4.20 ± 1.35‰) and from −4.30‰ to + 1.08‰ (mean: −1.03 ± 1.30‰), respectively.

4. DISCUSSION

4.1. T_{47} and its relationship to environmental temperature

For both *Bradybaena* and *Cathaica*, all the T_{47} values were higher than the MAT at the snail-inhabited sites, which is consistent with previous studies (Zaarur et al., 2011; Wang et al., 2016), but no correlation was observed between T_{47} and MAT (Fig. 3a). T_{47} remained within a certain range regardless of the ambient temperature increasing (Zaarur et al., 2011). Although the lowest T_{47} for *Cathaica* is ~ 2 °C higher than that for *Bradybaena* (i.e. 28.8 °C vs. 26.1 °C), they shared a common maximum T_{47} of approximately 35.5 °C. This suggests that 36 °C may be the threshold temperature for shell calcification for land snails. The highest T_{47} obtained by Zaarur et al. (2011) for modern land snails from a variety of localities throughout the world is 34 ± 3 °C. This agrees with other modern observations that indicate that an environmental temperature above 36 °C is lethal for land snails *Bradybaena* ravida (He et al., 2008). When we subtracted MAT from T_{47} to generate a temperature offset (T_{47}-MAT) and plotted the temperature offset and MAT together, an apparent negative correlation was found for both species (Fig. 3b). Specifically, the temperature offset uniformly decreased by ~0.8 °C per 1 °C MAT increase, i.e. −0.87 °C (T offset)/1 °C (MAT) for *Cathaica* and −0.81 °C (T offset)/1 °C (MAT) for *Bradybaena* (Fig. 3b). Similarly, the temperature offset gradient observed by Zaarur et al. (2011) was −0.77 °C per 1 °C MAT increase. This similarity in negative response reaffirms a common eco-physiological trait for land snails: that they tend to survive only during the warm season (i.e. summer) at a low MAT site, whereas an extended growing season is possible at a high MAT site. Moreover, snails may also modulate their body temperature through behavior (i.e. basking in the sun) at low MAT sites. This can be seen in a comparison of T_{47} at two extremely different MAT localities. For example, *Bradybaena* snails in Haerbin (in Northeast China), where the MAT is approximately 5 °C (with a June-July-August [JJA] temperature of 22.1 °C), have a T_{47} of ~33 °C; *Bradybaena* snails in Fuzhou (in southern China), where the MAT is approximately 20.5 °C (with a summer-months [JJA] temperature of 28.4 °C) have a T_{47} of ~29 °C. On this basis, we think the former T_{47} may represent the more likely summer temperature at the local site whereas the latter one reflects the average annual temperature. Therefore, to accurately determine the growth season for land snails at a site, it is essential to examine the relationship of T_{47} to the growing season temperature (GST).

The growing season of land snails at a specific site depends on a seasonal combination of ambient temperature and rainfall. In a monsoonal region, such as China, high temperatures and rainfall mainly occur during the summer months. However, the seasonal temperature gradient and duration of the rainy season vary from southern to northern China. For example, southern China is characterized by high air temperatures, abundant precipitation (generally more than 1000 mm/year), and more equitable distribution of rainfall throughout the year (Fig. 4c). In contrast, northern China experiences higher rainfall during the summer and a large annual temperature gradient (Fig. 4a). In this context, we divided our study area into three zones based on 10 °C and 20 °C MAT demarcations. The zone with MAT < 10 °C (Group 1) lies mainly in northeast and northwest China (north to 40 °N) and is an arid to semi-arid area with annual precipitation generally less than 500 mm and with more than 55 % of the rainfall occurring during the summer (JJA). Therefore, we assigned JJA as the main growing season for land snails in this area. The zone with an MAT between 10 °C and 20 °C (Group 2) in central and southern China is confined to a semi-humid to humid area with an annual precipitation between 500 mm and

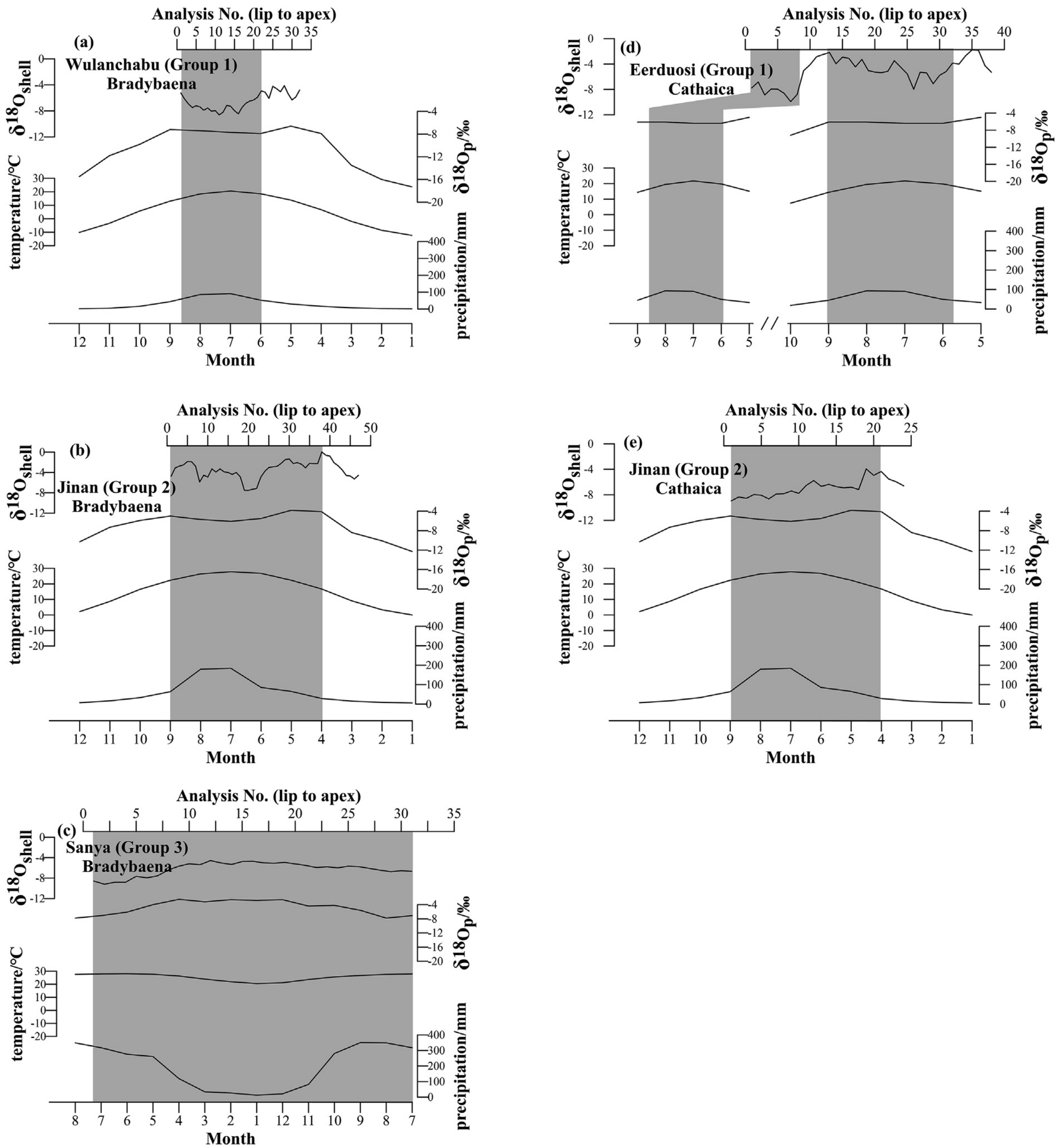

Fig. 4. A comparison of growth-band $\delta^{18}O_{shell}$ to the monthly distribution of $\delta^{18}O_p$, temperature, and precipitation at selected sites representative of each group of land snails. All $\delta^{18}O_{shell}$ curves are shown from shell lip to apex. The first data point sampled at the shell lip was adjusted to the expected latest shell-precipitation month based on shell collection time. The shells were respectively collected on (a) August 18th, 2016; (b) September 1st, 2016; (c) July 7th, 2014; (d) August 17th, 2016; and (e) September 1st, 2016. For most shells, the dip in the $\delta^{18}O_{shell}$ curve represents the summer months.

1900 mm, a monthly mean temperature > 10 °C, and a monthly rainfall > 20 mm for each warm month (April-October). In this case, April-October was considered as the land snails' growth season. The zone with a MAT > 20 °C (Group 3) is situated south of the Tropic of Cancer (23.5 °N), and is a sub-tropical area, with relatively high air temperature and abundant rainfall year-round (with an annual rainfall amount >1000 mm). The lowest monthly temperature is >10 °C and a minimum of 13 mm of rainfall occurs during January at Sanya. Arguably, land snails may secrete their shells throughout the year. Notably, some mountainous sites in Group 2 have higher rainfall than sites in Group 3, but the relatively low temperatures at these high-elevation sites prohibit the growth of land snails during the winter months.

To examine land snail growth seasonality in different regions in China, we measured $\delta^{13}C$ and $\delta^{18}O$ along the growth band on each *Bradybaena* and *Cathaica* shell from selected sites. We chose a single *Bradybaena* shell from Wulanchabu, Jinan, and Sanya that corresponds to Group 1, 2, and 3, respectively. As shown in Fig. 4a, shell $\delta^{18}O$ at Wulanchabu showed a U-shaped pattern (i.e. a concave curve) which corresponds with the effect of rainfall $\delta^{18}O$ during the summer months (JJA). In contrast, shell $\delta^{18}O$ at Jinan showed more significant seasonal changes in rainfall $\delta^{18}O$ including an amount effect during summer and a temperature effect during spring and autumn (Fig. 4b). In contrast to the aforementioned sites, shell $\delta^{18}O$ at Sanya showed a convex curve with a lower negative value in the center, indicating a nearly year-round growth from part of the summer to the previous summer month, as the snail was collected during August 2015 (Fig. 4c). For *Cathaica*, shell $\delta^{18}O$ at Eerdousi (Group 1) indicated significant rainfall $\delta^{18}O$ during two consecutive summer seasons, whereas shell $\delta^{18}O$ at Jinan (Group 2) recorded part of the summer and autumn seasons (Fig. 4d and e). The *Cathaica* shell at Jinan was too thin to sample near the apex thus some seasonal information was missed. Collectively, the oxygen isotopic data along the growth band of the single shells align with the assumed growth seasons for the three designated groups.

Based on the growing seasons, we examined the relationship of T_{47} with the environmental temperature. As shown in Fig. 5, there was a strong positive correlation of T_{47} with the growing season temperature (GST) for each group of *Bradybaena* and *Cathaica* land snails. Moreover, the positive correlation remained robust when we combined different groups within each species (Fig. 6). We compared the pooled data for each species to the clumped isotopes of biogenic carbonate published in previous studies. As shown in Fig. 6, all the T_{47} values of the *Bradybaena* and *Cathaica* land snails were systematically higher than the GST. The mean offset of *Bradybaena* T_{47} from the GST was 9.5 ± 1.4 °C whereas the mean difference between *Cathaica* T_{47} and the GST was 12.5 ± 1.4 °C. Comparing T_{47} between *Bradybaena* and *Cathaica* at the same site over 18 localities, we found that *Cathaica* had a T_{47} value 3.4 ± 1.5 °C higher than that of *Bradybaena*. This is consistent with a previous report based on eight sites on the Chinese Loess Plateau which found that *Cathaica* clumped isotope temperatures were 3–5 °C higher than those of *Bradybaena* (Wang et al., 2016). The discrepancy in T_{47} was attributed to the different eco-physiological traits of the two species (Wang et al., 2016). For example, we noticed in our land snail fieldwork collection that *Bradybaena* were inactive and stayed in the shady and damp litter layer under shrubs or trees, whereas *Cathaica* were more active and often climbed on trunks or twigs of trees. Therefore, *Cathaica* had higher potential exposure to sunlight thus enhancing their calcification temperature. Differences in shell color, thickness, and appearance between the two species lend support to this observation (Wang et al., 2016). An alternative explanation could be differences in the duration of the growing season of the two species, which could also produce such small offsets in temperature. However, intro-shell $\delta^{18}O$ variations (along the growth band) for *Bradybaena* and *Cathaica* at Jinan indicated that these species probably lived in the same season (Fig. 4b and e). In this

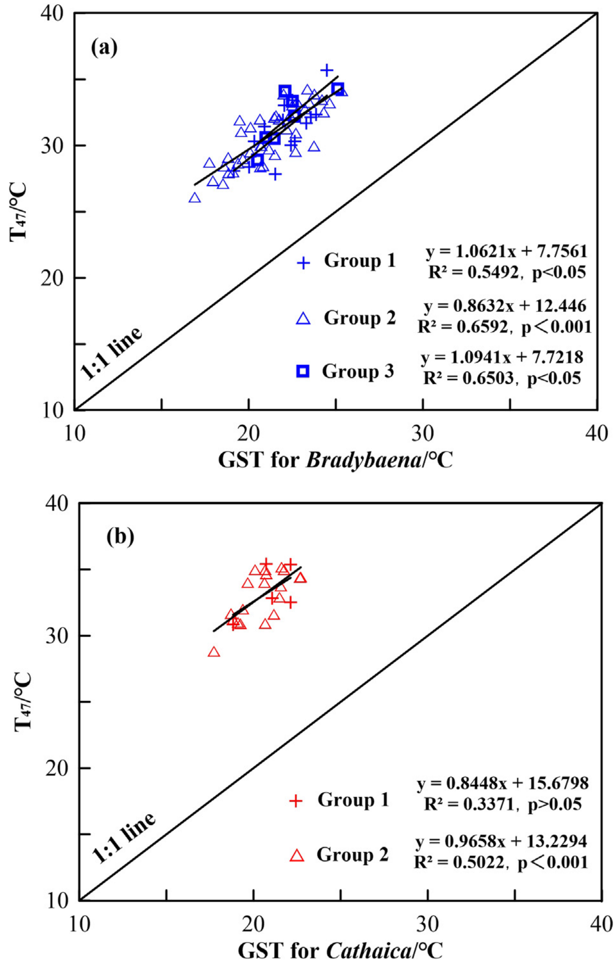

Fig. 5. Plots showing positive correlation between T_{47} and GST for (a) *Bradybaena* and (b) *Cathaica* in different MAT groups. Note the p value of Group 1 of *Cathaica* is above 0.05 because of the small number of sample sites (only 5 sites, see Table EA-2).

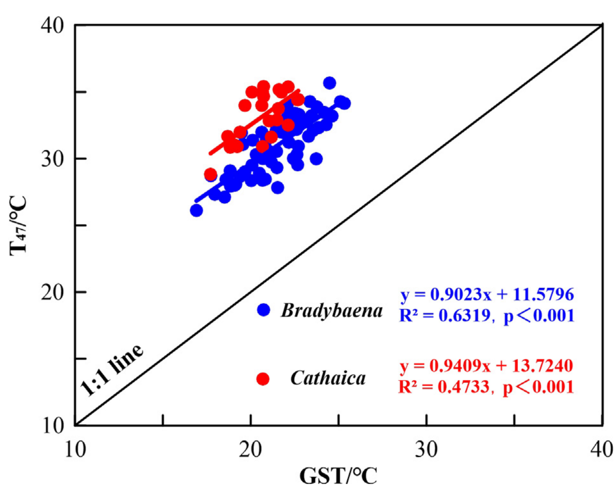

Fig. 6. Plot showing the positive correlation of T_{47} to GST for *Bradybaena* and *Cathaica*. All data were combined together for each species. The GST means growing season temperature.

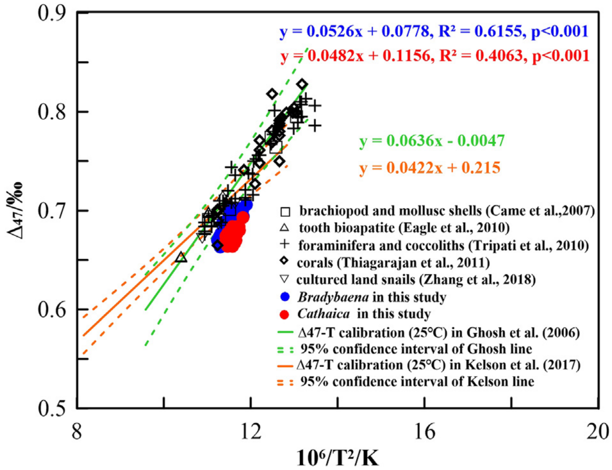

Fig. 7. Δ_{47}-T relationship for *Bradybaena* and *Cathaica* as compared to the Ghosh inorganic calibration line and other published data for biogenic carbonates. Only Δ_{47} data determined for biogenic carbonates digested at 25 °C were used to maintain consistency with our analytical method.

context, the two species should experience the same environmental temperatures but respond/record it differently through different eco-physiological adaptations.

For comparison, we plotted a Δ_{47}-ambient temperature plot together with clumped isotopic data of biogenic carbonates from previous studies and the calibration lines provided by Ghosh et al. (2006) and Kelson et al. (2017) (Fig. 7). Notably, most of the previously published Δ_{47} data were originally calibrated against stochastic distribution (i.e. heated gas line). To enable a direct comparison, we employed the recalibrated data relative to an absolute reference frame using secondary projection, as provided by Eagle et al. (2013b). We only selected the clumped isotopes for biogenic carbonates which were digested at 25 °C in order to maintain consistency in the samples. As shown, the Δ_{47} data for brachiopods and mollusks (Came et al., 2007), tooth bioapatites (Eagle et al., 2010), deep-sea corals (Thiagarajan et al., 2011), foraminifera and coccoliths (Tripati et al., 2010), and cultured land snails at certain temperatures (Zhang et al., 2018) all were on the Ghosh line but deviated from the Kelson line, particularly at lower temperatures. Zhang et al. (2018) suggest that the Δ_{47} of their cultured land snails correlated the Kelson line. This may be because only the clumped data for shells digested at 25 °C from Zhang et al. (2018) were used for the comparison. Moreover, the two calibration lines tend to be very close in the central temperature range (i.e. 20–30 °C at which the snails were cultured). In contrast, unlike these biogenic carbonates, our land snails *Bradybaena* and *Cathaica* were positioned below both the Ghosh line and the Kelson line and outside of the 95% confidence interval. This discrepancy was attributed to higher-than-mean-ambient-temperature calcification of land snail shells and not to isotopic disequilibrium in the clumped isotopes during precipitation of shell carbonate ('vital effect'), as discussed by Zaarur et al. (2011). Furthermore, Zhang et al. (2018) also ruled out the vital effect in clumped isotopes because the Δ_{47} values of the land snail *Acusta despecta* cultured at known temperatures corresponded well with culturing temperatures. Moreover, if there is a vital effect, Δ_{47} and $\delta^{18}O$ in shell carbonate would change concurrently (Zaarur et al., 2011; Zhang et al., 2018), and there is no such trend observed (Fig. EA-1) which indicates the absence of a clumped isotopic vital effect in our land snail shells. Therefore, the recorded Δ_{47} temperatures (T_{47}) represent the temperatures the land snails are experiencing and land snails are active in microenvironment or days that are higher than mean seasonal temperature. Eagle et al. (2013a) also suggested a relationship between optimal growth and warmer seasons based on a good correlation of T_{47} from modern *Cathaica* sp. with warm-month daily high temperatures. However, Zhang et al. (2018) show that optimal growth in land snails corresponded with the culturing temperatures, as the growth temperature was controlled. Despite the higher calcification temperature of wild land snails, the stable offset allows us to determine the mean seasonal temperature of snail growth. We developed a transfer function of Δ_{47} for growth temperature for each of the two land snail species as follows:

$$\textit{Bradybaena}\ \Delta_{47} = (0.0526 \pm 0.0054) \times 10^6/T^2 + (0.0778 \pm 0.0618), \quad R^2 = 0.6155 \tag{2}$$

$$\textit{Cathaica}\ \Delta_{47} = (0.0482 \pm 0.0124) \times 10^6/T^2 + (0.1156 \pm 0.1440), \quad R^2 = 0.4063 \tag{3}$$

where Δ_{47} is in ‰ and T is in Kelvin degrees. The calibration temperature range is 16.9–25.3 °C for *Bradybaena* and 17.7–22.7 °C for *Cathaica*. It is recognized that land snail shells only integrate climatic information over a short time period and record species-specific or inter-location (habitat) effects. To eliminate the micro-environmental effect on land snail living habits and calcification temperature (namely Δ_{47}), we averaged Δ_{47} values for each group of study sites that have growth season temperature differences within 0.5 °C. On this basis, the correlation of Δ_{47} to GST largely improved for both species (Fig. EA-2). The refined transfer functions are as follows:

$$\textit{Bradybaena}\ \Delta_{47} = (0.0513 \pm 0.0036) \times 10^6/T^2 + (0.0930 \pm 0.0413), \quad R^2 = 0.9360 \tag{4}$$

$$\textit{Cathaica}\ \Delta_{47} = (0.0552 \pm 0.0111) \times 10^6/T^2 + (0.0351 \pm 0.1293), \quad R^2 = 0.8036 \tag{5}$$

The calibration slopes for these two functions (0.0513 and 0.0552) are apparently different from those of the Ghosh line and the Kelson line (i.e. 0.0636 and 0.0422, respectively). Nevertheless, they are fairly near the slope of 0.0559 for the compiled biogenic carbonates performed at 25 °C acid digestion (Eagle et al., 2013b), suggesting a similar temperature sensitivity.

4.2. Calculated $\delta^{18}O$ of snail body water and its relation to oxygen isotopes from precipitation

As previously mentioned, the $\delta^{18}O$ of snail body water ($\delta^{18}O_{BW}$) can be calculated based on snail shell $\delta^{18}O$ and Δ_{47}-derived temperature. To do this, we adopted the temperature-dependent oxygen isotope fractionation function developed by Kim et al. (2007):

$$1000\ln\alpha_{aragonite-water} = 17.88 \pm 0.13(10^3/T) - 31.14 \pm 0.46 \quad (6)$$

where T (in K) is the clumped isotopic temperature for each species.

The calculated $\delta^{18}O_{BW}$ for *Bradybaena* ranged from −4.47‰ to +3.80‰ whereas that of *Cathaica* varied from −4.30‰ to +1.08‰. A comparison of $\delta^{18}O_{BW}$ with the monthly weighted $\delta^{18}O$ of local precipitation (data obtained from http://www.waterisotopes.org and referred to in Bowen and Revenaugh (2003)) during the land snail growth season ($\delta^{18}O_{P\text{-}GS}$), showed that the snail body water of both species was enriched in ^{18}O relative to seasonal precipitation during land snail growth (Fig. 8a). This is consistent with previous studies regarding land snail oxygen isotopes at a variety of sites (Baldini et al., 2007; Goodfriend and Ellis, 2002; Goodfriend et al., 1989; Lécolle, 1985; Prendergast et al., 2015; Yanes et al., 2009; Zanchetta et al., 2005) and the snail evaporative flux-balance mixing model (Balakrishnan and Yapp, 2004). An explanation for such enrichment in ^{18}O is that the meteoric water has undergone intense evaporation before being ingested by land snails (Balakrishnan and Yapp, 2004). Our T_{47} results showed that *Bradybaena* and *Cathaica* land snails precipitated their shell carbonates at temperatures at least 10 °C higher than the mean GST. This high temperature would have enhanced the effect of evaporation on the oxygen isotopes of land snail body water.

Meanwhile, a weak positive correlation between $\delta^{18}O_{BW}$ and $\delta^{18}O_{P\text{-}GS}$ was observed for *Bradybaena*, but no correlation was observed for *Cathaica* (Fig. 8a). Moreover, when we subdivided the study area into two parts (i.e. southern and northern China), the correlation between $\delta^{18}O_{BW}$ and $\delta^{18}O_{P\text{-}GS}$ for *Bradybaena* was enhanced and a more robust correlation emerged in northern China (Fig. 8b). The reason for the lack of $\delta^{18}O_{BW}$-$\delta^{18}O_{P\text{-}GS}$ correlation for *Cathaica* may lie in its eco-physiological traits. As previously mentioned, *Cathaica* is a more active species and they often climb on trunks or twigs of trees to feed on leaves. *Cathaica*, therefore, has a higher possibility of exposure to sunlight, which strongly evaporates snail body water and results in $\delta^{18}O_{BW}$ deviation from $\delta^{18}O_{P\text{-}GS}$. *Cathaica* is able to obtain water from a variety of sources such as tree/grass leaves, organic litter, soil water, dew water, and rainwater. This would complicate the oxygen isotopic composition of the snail body water. Collectively, the $\delta^{18}O_{BW}$ of *Cathaica* tended to be less tightly linked to $\delta^{18}O_{P\text{-}GS}$. In contrast, *Bradybaena* are inactive and usually stay in the shady and damp litter layer under shrubs/trees. This could protect *Bradybaena* body water from strong evaporation and allow *Bradybaena* to retain as much soil moisture as possible. In this case, the *Bradybaena* body water eventually bears the isotopic signature of precipitation during their growth season. At the same time, we also obtained a more robust correlation of $\delta^{18}O_{BW}$ to $\delta^{18}O_{P\text{-}GS}$ for *Bradybaena* in northern China than those in southern China. This is because most rainfall occurs during the summer months in northern China with intense rainfall events which can effectively

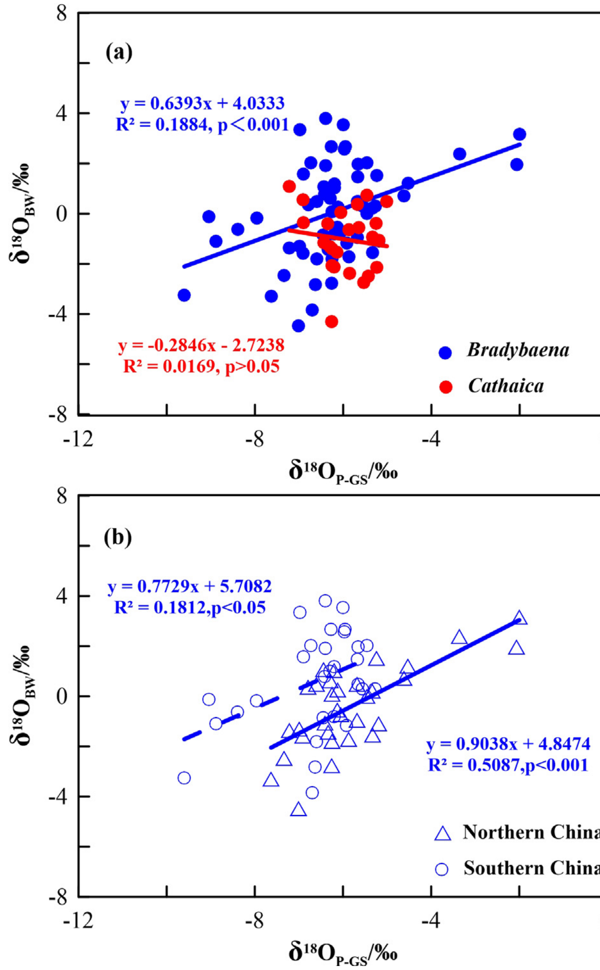

Fig. 8. Comparison of $\delta^{18}O_{BW\text{-}T47}$ to $\delta^{18}O_p$ for two land snail species. (a) All data for *Bradybaena* and *Cathaica* for the whole of China. (b) Data for *Bradybaena* was sub-divided into northern and southern China.

reduce the effect of evaporation and maintain the original $\delta^{18}O_{P\text{-}GS}$ signal in the soil moisture. Furthermore, the relatively low temperatures in northern China also contribute to low evaporation. In contrast, in southern China, the more equitably distributed rainfall throughout the year and relatively high temperatures would result in enhanced evaporation of rainwater (and thus enrichment in ^{18}O) before it is ingested by land snails. This is indicated by the higher $\delta^{18}O_{BW}$ for *Bradybaena* in southern China than for those in northern China under the same $\delta^{18}O_{P\text{-}GS}$ conditions (Fig. 8b). In brief, the reconstructed $\delta^{18}O_{BW}$ for *Bradybaena* can serve as an indicator of rainfall $\delta^{18}O$, particularly in northern China, and holds the potential to trace hydrological changes.

4.3. Application to paleo-temperature reconstruction

In a previous study, Eagle et al. (2013a) analyzed clumped isotopes on *Cathaica* sp. shell carbonate and reconstructed summertime (JJA) daily high temperatures using measured Δ_{47} values and the Ghosh line. The reconstructed summer daily maximum temperature was 31.2 ± 1.5 °C and 24.2 ± 1.9 °C during the present day and LGM, respectively. However, the postulated GST needs to be reconsidered because we constructed Δ_{47}-T as a transfer function for *Cathaica*. The Δ_{47} values provided by Eagle et al. (2013a) were calibrated against stochastic distribution (i.e. heated gas line), under which reference scale the Δ_{47} for Carrara Marble was approximately 0.352‰. Nevertheless, the Δ_{47} for Carrara Marble on the absolute reference frame was approximately 0.395‰ (Dennis et al., 2011). Therefore, an offset of 0.043‰ was added to the original Δ_{47} values to calibate with our transfer function. The resultant Δ_{47} was 0.662 ± 0.006‰ and 0.692 ± 0.008‰ for modern and glacial land snails, respectively. Using our transfer function (5), the calculated temperature was accordingly 23.0 ± 1.5 °C and 16.2 ± 1.9 °C. Because the MAT at the study site is below 10 °C, the aforementioned Δ_{47}-derived temperatures represent the summer (JJA) average. In fact, the obtained mean summer temperature of 23.0 ± 1.5 °C is nearly identical to that of the modern observation (23.3 ± 1.1 °C). This testifies to the validity of our land snail Δ_{47}-T transfer function. Moreover, the reconstructed LGM mean summer temperature using land snails (16.2 ± 1.9 °C) is fairly close to that of the soil carbonate nodule Δ_{47}-derived value (i.e. 17.8 ± 2.0 °C in Eagle et al. (2013a)), which indicates the warm-month mean temperature. In addition, the reconstructed drop in mean summer temperature during the LGM compared to the present was approximately 6.8 ± 2.4 °C. This further confirms the model-simulated 6.7 °C and 8.8 °C cooling on the Chinese Loess Plateau during the LGM when considering the stationary wave response to continental ice sheets (Eagle et al., 2013a).

5. CONCLUSION

In this study, we systematically analyzed clumped isotopes (Δ_{47}) for two common land snail species (*Bradybaena* and *Cathaica*) in China with the objective of developing a Δ_{47}-T transfer function. The temperatures calculated using the Δ_{47} (T_{47}) of both species were maintained within a certain range and showed no correlation with MATs at the study sites. However, the T_{47}-MAT offset was negatively correlated to MAT, suggesting that land snails tend to survive in warmer months (summer) at cold sites. Meanwhile, snails may also increase their body temperature through behavior (i.e. basking in the sun) at low MAT sites. After assigning an appropriate growth season period to land snails living in different parts of China, a robust correlation emerged between Δ_{47}-derived temperature and GST. We, therefore, constructed Δ_{47}-GST transfer functions for both *Bradybaena* and *Cathaica* land snails. The function for *Cathaica* was successfully applied to reconstruct mean summer (JJA) temperatures during the LGM and modern times on the central Chinese Loess Plateau based on Δ_{47} data of *Cathaica* sp. provided by Eagle et al (2013a). This testifies to the validity of our constructed transfer function. Nevertheless, clumped temperatures of *Cathaica* are 3.4 ± 1.5 °C higher than those of *Bradybaena* at 18 sites containing both land snails, indicating that a species-specific transfer function is needed for reconstructing paleotemperature using land snail clumped isotopes. In addition, the calculated $\delta^{18}O$ of body water ($\delta^{18}O_{BW}$) for *Bradybaena* showed a robust correlation with rainfall $\delta^{18}O$ particularly in northern China and holds the potential to trace hydrological changes in the region.

ACKNOWLEDGMENTS

This study was supported by the National Natural Science Foundation of China (Grant No. 41572163), Strategic Priority Research Program of the Chinese Academy of Sciences (Grant No. XDB26000000 and XDA19050104), and State Scholarship Fund for Study Abroad by the China Scholarship Council (CSC). We would like to thank Prof. Deniu Chen for identifying the land snail species and Prof. Jay Quade and two anonymous reviewers for their constructive comments that greatly improved early version of the manuscript. The China Meteorological Data Service Center provided the meteorological data for our study sites.

APPENDIX A. SUPPLEMENTARY MATERIAL

Supplementary data to this article can be found online at https://doi.org/10.1016/j.gca.2019.04.028.

REFERENCES

Balakrishnan M. and Yapp C. J. (2004) Flux balance models for the oxygen and carbon isotope compositions of land snail shells. *Geochim. Cosmochim. Acta* **68**, 2007–2024.

Baldini L. M., Walker S. E., Railsback L. B., Baldini J. U. L. and Crowe D. E. (2007) Isotopic ecology of the modern land snail Cerion, San Salvador, Bahamas: Preliminary advances toward establishing a low-latitude island paleoenvironmental proxy. *Palaios* **22**, 174–187.

Bowen G. J. and Revenaugh J. (2003) Interpolating the isotopic composition of modern meteoric precipitation. *Water. Resour. Res.* **39**, 3178–3184.

Came R. E., Eiler J. M., Veizer J., Azmy K., Brand U. and Weidman C. R. (2007) Coupling of surface temperatures and atmospheric CO_2 concentrations during the Palaeozoic era. *Nature* **449**, 198–202.

Cui L. L. and Wang X. (2014) Determination of clumped isotopes in carbonate using isotope ratio mass spectrometer: Effects of extraction potential and long-term stability. *Int. J. Mass. Spectrom.* **372**, 46–50.

DeNiro M. J. and Epstein S. (1978) Influence of diet on the distribution of carbon isotopes in animals. *Geochim. Cosmochim. Acta* **42**, 495–506.

Dennis K. J., Affek H. P., Passey B. H., Schrag D. P. and Eiler J. M. (2011) Defining an absolute reference frame for 'clumped' isotope studies of CO_2. *Geochim. Cosmochim. Acta* **75**, 7117–7131.

Eagle R. A., Risi C., Mitchell J. L., Eiler J. M., Seibt U., Neelin J. D., Li G. J. and Tripati A. K. (2013a) High regional climate sensitivity over continental China constrained by glacial-recent changes in temperature and the hydrological cycle. *PNAS* **110**, 8813–8818.

Eagle R. A., Eiler J. M., Tripati A. K., Ries J. B., Freitas P. S., Hiebenthal C., Wanamaker A. D., Taviani M., Elliot M., Marenssi S., Nakamura K., Ramirez P. and Roy K. (2013b) The influence of temperature and seawater carbonate saturation state on $^{13}C^{18}O$ bond ordering in bivalve mollusks. *Biogeosciences* **10**, 4591–4606.

Eagle R. A., Schauble E. A., Tripati A. K., Tutken T., Hulbert R. C. and Eiler J. M. (2010) Body temperatures of modern and extinct vertebrates from ^{13}C–^{18}O bond abundances in bioapatite. *PNAS* **107**, 10377–10382.

Francey R. (1983) A comment on 13C/12C in land snail shells. *Earth. Planet. Sc. Lett.* **63**, 142–143.

Ghosh P., Adkins J., Affek H., Balta B., Guo W. F., Schauble E. A., Schrag D. and Eller J. M. (2006) ^{13}C–^{18}O bonds in carbonate minerals: A new kind of paleothermometer. *Geochim. Cosmochim. Acta* **70**, 1439–1456.

Goodfriend G. A. and Ellis G. L. (2002) Stable carbon and oxygen isotopic variations in modern Rabdotus land snail shells in the southern Great Plains, USA, and their relation to environment. *Geochim. Cosmochim. Acta* **66**, 1987–2002.

Goodfriend G. A., Magaritz M. and Gat J. R. (1989) Stable isotope composition of land snail body water and its relation to environmental waters and shell carbonate. *Geochim. Cosmochim. Acta* **53**, 3215–3221.

Grossman E. L. and Ku T.-L. (1986) Oxygen and carbon isotope fractionation in biogenic aragonite: temperature effects. *Chem. Geol.: Isotope Geosci. Sect.* **59**, 59–74.

He T., Xu P., Qiang J. and Dong Y. (2008) Effects of temperature and humidity on Bradybaena ravida. *J. Changjiang Vegetables* **2**, 54–55 (in Chinese).

Kelson J. R., Huntington K. W., Schauer A. J., Saenger C. and Lechler A. R. (2017) Toward a universal carbonate clumped isotope calibration: diverse synthesis and preparatory methods suggest a single temperature relationship. *Geochim. Cosmochim. Acta* **197**, 104–131.

Kim S. T., O'Neil J. R., Hillaire-Marcel C. and Mucci A. (2007) Oxygen isotope fractionation between synthetic aragonite and water: Influence of temperature and Mg^{2+} concentration. *Geochim. Cosmochim. Acta* **71**, 4704–4715.

Lécolle P. (1985) The oxygen isotope composition of land snail shells as a climatic indicator: applications to hydrogeology and paleoclimatology. *Chem. Geol.: Isotope Geosci. Sect.* **58**, 157–181.

Lozek V. (1965) The loess environment in central Europe. In *Loess and related Eolian Deposits of the world, prceedings 7th INQUA Congress* (eds. C. Schultz and J. C. Frye). University of Nebraska Press, Boulder, Lincoln, pp. 67–80.

Liu T. S. et al. (1985) *Loess and the Environment*. Science Press, Beijing, pp. 169–170.

Liu Z. X., Gu Z. Y., Xu B. and Wu N. Q. (2006) Monsoon precipitation effect on oxygen isotope composition of land snail shell carbonate from the Loess Plateau. *Quaternary Sci.* **26**, 643–648 (in Chinese).

Liu Z. X., Gu Z. Y., Wu N. Q. and Xu B. (2007) Diet control on carbon isotopic composition of land snail shell carbonate. *Chin. Sci. Bull.* **52**, 388–394.

Magaritz M., Heller J. and Volokita M. (1981) Land-air boundary environment as recorded by the ^{18}O/^{16}O and ^{13}C/^{12}C isotope ratios in the shells of land snails. *Earth. Planet. Sc. Lett.* **52**, 101–106.

Mccrea J. M. (1950) On the isotopic chemistry of carbonates and a paleotemperature scale. *J. Chem. Phys.* **18**, 849–857.

Metref S., Rousseau D.-D., Bentaleb I., Labonne M. and Vianey-Liaud M. (2003) Study of the diet effect on δ^{13}C of shell carbonate of the land snail *Helix aspersa* in experimental conditions. *Earth. Planet. Sci. Lett.* **211**, 381–393.

Prendergast A. L., Stevens R. E., Barker G. and O'Connell T. C. (2015) Oxygen isotope signatures from land snail *(Helix melanostoma)* shells and body fluid: Proxies for reconstructing Mediterranean and North African rainfall. *Chem. Geol.* **409**, 87–98.

Sparks B. W. (1961) The ecologcal interpretation of quaternary non-marine mollusca. *Proc. Linnean Soc. London* **172**, 71–80.

Stott L. D. (2002) The influence of diet on the δ^{13}C of shell carbon in the pulmonate snail *Helix aspersa*. *Earth. Planet. Sc. Lett.* **195**, 249–259.

Thiagarajan N., Adkins J. and Eiler J. (2011) Carbonate clumped isotope thermometry of deep-sea corals and implications for vital effects. *Geochim. Cosmochim. Acta* **75**, 4416–4425.

Tripati A. K., Eagle R. A., Thiagarajan N., Gagnon A. C., Bauch H., Halloran P. R. and Eiler J. M. (2010) ^{13}C–^{18}O isotope signatures and 'clumped isotope' thermometry in foraminifera and coccoliths. *Geochim. Cosmochim. Acta* **74**, 5697–5717.

Wang X., Cui L. L., Zhai J. X. and Ding Z. L. (2016) Stable and clumped isotopes in shell carbonates of land snails *Cathaica* sp. and *Bradybaena* sp. in north China and implications for ecophysiological characteristics and paleoclimate studies. *Geochem., Geophys., Geosyst.* **17**, 219–231.

Wu N. Q., Li F. J. and Rousseau D. D. (2018) Terrestrial mollusk records from Chinese loess sequences and changes in the East Asian monsoonal environment. *J. Asian. Earth. Sci.* **155**, 35–48.

Yanes Y., Romanek C. S., Delgado A., Brant H. A., Noakes J. E., Alonso M. R. and Ibanez M. (2009) Oxygen and carbon stable isotopes of modern land snail shells as environmental indicators from a low-latitude oceanic island. *Geochim. Cosmochim. Acta* **73**, 4077–4099.

Yapp C. J. (1979) Oxygen and carbon isotope measurements of land snail shell carbonate. *Geochim. Cosmochim. Acta* **43**, 629–635.

Zaarur S., Olack G. and Affek H. P. (2011) Paleo-environmental implication of clumped isotopes in land snail shells. *Geochim. Cosmochim. Acta* **75**, 6859–6869.

Zanchetta G., Leone G., Fallick A. and Bonadonna F. (2005) Oxygen isotope composition of living land snail shells: data from Italy. *Palaeogeography, Palaeoclimatol., Palaeoecol.* **223**, 20–33.

Zhang N., Yamada K., Kano A., Matsumoto R. and Yoshida N. (2018) Equilibrated clumped isotope signatures of land-snail shells observed from laboratory culturing experiments and its environmental implications. *Chem. Geol.* **488**, 189–199.

Associate editor: Jay Quade